The carbonatation of gypsum: Pathways and pseudomorph formation

LURDES FERNÁNDEZ-DÍAZ,[1,*] CARLOS M. PINA,[1] JOSÉ MANUEL ASTILLEROS,[1] AND NURIA SÁNCHEZ-PASTOR[2]

[1]Departamento de Cristalografía y Mineralogía, Universidad Complutense de Madrid, Madrid 28040, Spain
[2]Department für Geo- und Umweltwissenschaften, Ludwig-Maximilians-Universität, Munich 80333, Germany

ABSTRACT

In this paper, we present an experimental study of the interaction between gypsum (010) surfaces and aqueous solutions of Na_2CO_3 with different concentrations. This interaction leads to the carbonatation (i.e., the transformation into carbonate minerals) of gypsum crystals, which under ambient conditions shows the characteristics of a mineral replacement and leads to the formation of pseudomorphs consisting of an aggregate of calcite crystals. Carbonatation progress was monitored by scanning electron microscopy (SEM) and glancing incidence X-ray diffraction (GIXRD). The carbonatation advances from outside to inside the gypsum crystal and occurs through a sequence of reactions, which involves the dissolution of gypsum and the simultaneous crystallization of different polymorphs of $CaCO_3$ [amorphous calcium carbonate (ACC), vaterite, aragonite, and calcite], as well as several solvent-mediated transformations between these polymorphs. The sequence in which $CaCO_3$ phases form is interpreted taking into consideration nucleation kinetics and the qualitative evolution of several chemical parameters in the aqueous solution. The textural characteristics of the transformed regions are described. The degree of faithfulness of the pseudomorphs obtained is related to the kinetics of the carbonatation process, which in turn depends on the initial concentration of carbonate in the aqueous solutions. Finally, changes in the rate at which the transformation front advances are discussed on the basis of both textural and physicochemical considerations.

Keywords: Carbonatation, dissolution-crystallization, mineral replacement, gypsum, calcium carbonate, pseudomorphism

INTRODUCTION

Carbonate and evaporite deposits are intimately related in many different geological settings. Moreover, the transition of evaporites to carbonates is a common diagenetic process, which results from the transformation of relatively soluble evaporite minerals into more stable phases under specific physicochemical conditions (Rouchy et al. 2001). In particular, the carbonatation (i.e., the transformation into carbonate minerals) of evaporitic calcium sulfates (anhydrite and gypsum) has led to the formation of significant carbonate deposits, as pointed out by numerous authors (Wigley 1973; Kirkland and Evans 1976; McKenzie et al. 1980; Pierre and Rouchy 1988; Bell 1989; Youssef 1989; Anadón et al. 1992; Rouchy et al. 1994, 1998; Cañaveras et al. 1996, 1998; Sanz-Rubio et al. 2001). Two main mechanisms have been invoked to explain the carbonatation of gypsum. One involves bacterial sulfate reduction in organic-rich sediments and leads to the formation of native sulfur accumulations (Anadón et al. 1992). The other one assumes that the carbonatation occurs as a result of sulfate dissolution by meteoric carbonate-rich groundwaters (Wigley 1973; Pierre and Rouchy 1988). This second mechanism has been unequivocally identified from stable isotope data in several sedimentary basins (Sanz-Rubio et al. 2001). In both cases, pseudomorphs of calcite or aragonite after gypsum, as well as gypsum relicts, have been observed randomly distributed within sediment layers.

* E-mail: lfdiaz@geo.ucm.es

Deep in the Earth's crust and in the mantle, under high temperatures and/or pressures, transformations can take place via solid-state reactions. However, on the Earth's surface and at typical sediment temperatures, solid-state processes are kinetically hindered and their contribution to most mineral transformations can be considered negligible. Under these conditions, the presence of aqueous solutions provides an efficient mass-transfer medium. Thus, mineral transformations can occur at a substantially accelerated rate (Wang and Morse 1996) through the combination of two processes: the dissolution of the reactant phase and the crystallization of the new one (Carmichael 1969; Cardew and Davey 1985; Wang et al. 1995; Pina et al. 2000). These transformations frequently show the characteristics of mineral replacements (Putnis 2002), i.e., the volume and the shape of the reactant crystals are preserved during the transformation. This implies that the dissolution of the reactant and the crystallization of the product phase (or phases) necessarily occur simultaneously and at coupled rates (Harlov et al. 2007; Putnis et al. 2007a; Oelkers et al. 2007). Moreover, the formation of pseudomorphs normally occurs (Putnis et al. 2006, 2007b; Putnis and Putnis 2007; Sánchez-Pastor et al. 2007). Under certain circumstances, pseudomorphization can be extremely faithful to both the shape and the surface features of the original crystal, which are precisely preserved.

The early work by Flörke and Flörke (1961) reported for the first time the characteristics of the transformation of gypsum into vaterite/calcite under laboratory controlled conditions. Despite

the fact that the transformation of sulfates into carbonates has evident implications for carbonate sedimentology and, furthermore, is involved in the global geochemical cycle of carbon, few efforts have been made to experimentally approach this type of process. Thus, the microscopic mechanisms involved in the carbonatation of gypsum remain poorly understood. In this paper, we present an experimental study of the transformation of gypsum into $CaCO_3$ as a result of reaction with carbonate-bearing aqueous solutions. Since the dissolution-crystallization reactions involved in the carbonatation process occur at the crystal-fluid interface, we have focused our research on the gypsum (010) face, which is the most important one morphologically, and contributes about 75% of the total surface area of gypsum crystals grown from pure aqueous solutions of $CaSO_4$ (Simon and Bienfait 1965). Our research follows the progress of the carbonatation process by monitoring the movement of the reaction front perpendicular to an (010) gypsum surface and studies the evolution of the mineralogy and the textural characteristics of the transformed region. Furthermore, we relate the kinetics of the carbonatation to both the thickness and texture of the transformed layer and the evolution of basic physicochemical parameters. As such, we have established general conclusions about the factors controlling the progress of the carbonatation of gypsum.

Experimental methods

A series of experiments were carried out by submerging optically clear gypsum crystals (Teruel, Spain) cleaved on (010) faces in 1 mL volumes of Na_2CO_3 aqueous solutions in vessels closed with a polypropylene cap to avoid contact with the atmosphere and evaporation. X-ray fluorescence spectroscopy (XRF) and X-ray diffraction (XRD) analysis confirmed that the starting material corresponded to highly pure gypsum (less than 0.2 wt% impurities, mainly Na, Sr, and P). The size of the gypsum crystals was about 3 × 3 × 0.8–1 mm. Since gypsum crystals show a preferential cleavage on (010), most of the surface area exposed to the carbonate aqueous solutions corresponded to this face. Four Na_2CO_3 solution concentrations were used: 0.5, 0.25, 0.1, and 0.05 *M*. In the high concentration case, a commercial 0.5 mol/L Na_2CO_3 solution (Reidel de Häen) was directly used, whereas for the rest, solutions were prepared by diluting the commercial solution in high purity deionized water (resistivity: 18 MΩ·cm).

Independent experimental runs were carried out for each Na_2CO_3 aqueous solution concentration. Gypsum crystals were removed from the solutions after different reaction periods, ranging from 1 min to 15 days. In all cases, partially to totally replaced crystals were dried rapidly by blowing pressurized air on their surfaces. All experiments were carried out in a thermostated room at 25 ± 0.5 °C and atmospheric pressure. Each run was repeated at least three times to quantify the variability of the measurements.

The crystals were studied by glancing incidence X-ray diffraction (GIXRD) and scanning electron microscopy (SEM). X-ray diffraction patterns were used to identify the different $CaCO_3$ phases formed during the replacement process. The diffractometer used was a PANalytical X'Pert PRO MRD equipped with a Cu*K*α X-ray source, an X-ray parabolic mirror in the incident beam, and a parallel plate collimator with flat graphite monochromator in the diffracted beam (Xe proportional detector). The small angle of incidence (0.5°) allows one to obtain information corresponding to the shallower layers, minimizing the presence of peaks coming from the bulk of the gypsum crystal. This information allowed us to determine the sequence of $CaCO_3$ phases formed at different stages of the transformation. Both the (010) surface and sections cut perpendicular to this face of the partially transformed gypsum crystals were imaged by SEM (JEOL JSM 6400, 40 kV). SEM images of the gypsum (010) surfaces provided information about textural and mineralogical features. Measurements on images of the perpendicular sections of the samples removed from the Na_2CO_3 solutions at different times allowed us to quantify the rate of advancement of the carbonatation front. The volume, as well as the number of moles, of gypsum that have passed to the solution at any time along the process can be approximately estimated from the thickness of the transformed layer, considering an average area for the (010) surface of the gypsum crystal exposed to the solution of 8 ± 0.5 mm^2. These data were used to model the evolution of the saturation index with respect to gypsum ($Ksp_{gypsum} = 10^{-4.58}$) with time, as well as the evolution of the concentration of CO_3^{2-} and SO_4^{2-} ions in the aqueous solution, considering times subsequent to the first appearance of calcite. This modeling was done using the geochemical code PHREEQC (Parkhurst and Appelo 2000). The initial Na_2CO_3 concentration of the aqueous solution, equilibrated with atmospheric CO_2, was used as input datum. Then, the tool "Reaction," considering gypsum as the reactant, was applied. This tool operates through reaction steps. In each step, the solution was equilibrated with both atmospheric CO_2 and calcite, using the "Equilibrium" tool of PHREEQC. A total number of 70 reaction steps were defined.

Results

Mineralogical and textural evolution during the carbonatation process

The combination of GIXRD diffractograms (Fig. 1) with SEM images (Figs. 2–6) obtained after different periods of exposure of the gypsum (010) surface to the Na_2CO_3 solutions allow us to monitor the mineralogical and textural evolution of the transformed layer. Reactions on the gypsum (010) surface begin immediately after immersion of crystals into an aqueous solution of Na_2CO_3, independent of its initial concentration. However, the results obtained show that the sequence of reactions depends on the initial concentration of the aqueous solution. In the experiments carried out using 0.5 *M* Na_2CO_3 solutions, SEM images show that after 1 min a thin layer (1 μm thick), resulting from the coalescence of nanometric spheres (diameter: 300–400 nm), completely carpets the gypsum (010) surface (Fig. 2). This layer progressively becomes thicker and more compact, with formation of "bottle necks" between the spheres. The corresponding GIXRD diffractogram only shows peaks that match those of gypsum, indicating that this first layer most probably consists of the amorphous calcium carbonate (phase ACC). In contrast, the diffractograms corresponding to slightly longer reaction periods show several peaks that match either vaterite (5 min) or vaterite and calcite (15 min). For reaction periods longer than 45 min, these two phases are clearly distinguishable in the SEM images (Figs. 3a and 3b). Whereas vaterite appears as rounded aggregates with an equatorial cleft and a very rough surface, calcite crystals show the common rhombohedral habit, with signs of dendritic growth. As can be seen in Figure 3, ACC still remains as the main phase in the transformed region for a reaction period of 45 min. However, the ACC layer has clearly dissolved around vaterite aggregates and calcite crystals, which indicates that a secondary dissolution-recrystallization process between $CaCO_3$ phases occurs locally. Moreover, the dissolution rate of gypsum seems to be increased by the presence of vaterite and/or calcite, as evidenced by the surface depressions formed around the points where crystals of these phases have developed. Similarly, in those areas where vaterite and calcite are in contact, vaterite aggregates have dissolved, whereas calcite crystals have grown (Fig. 3b). For reaction periods over 180 min, the original ACC layer has completely disappeared and the transformed region consists of an aggregate of calcite rhombohedra, with a minor amount of vaterite spherulites. After 24 h, the whole volume of the original gypsum fragment has completely transformed into $CaCO_3$. Although SEM images show that calcite is the main phase, XRD patterns indicate that vaterite is still present. Finally, after a week in contact with the solution, only calcite is detected.

When the starting concentration of the Na_2CO_3 aqueous

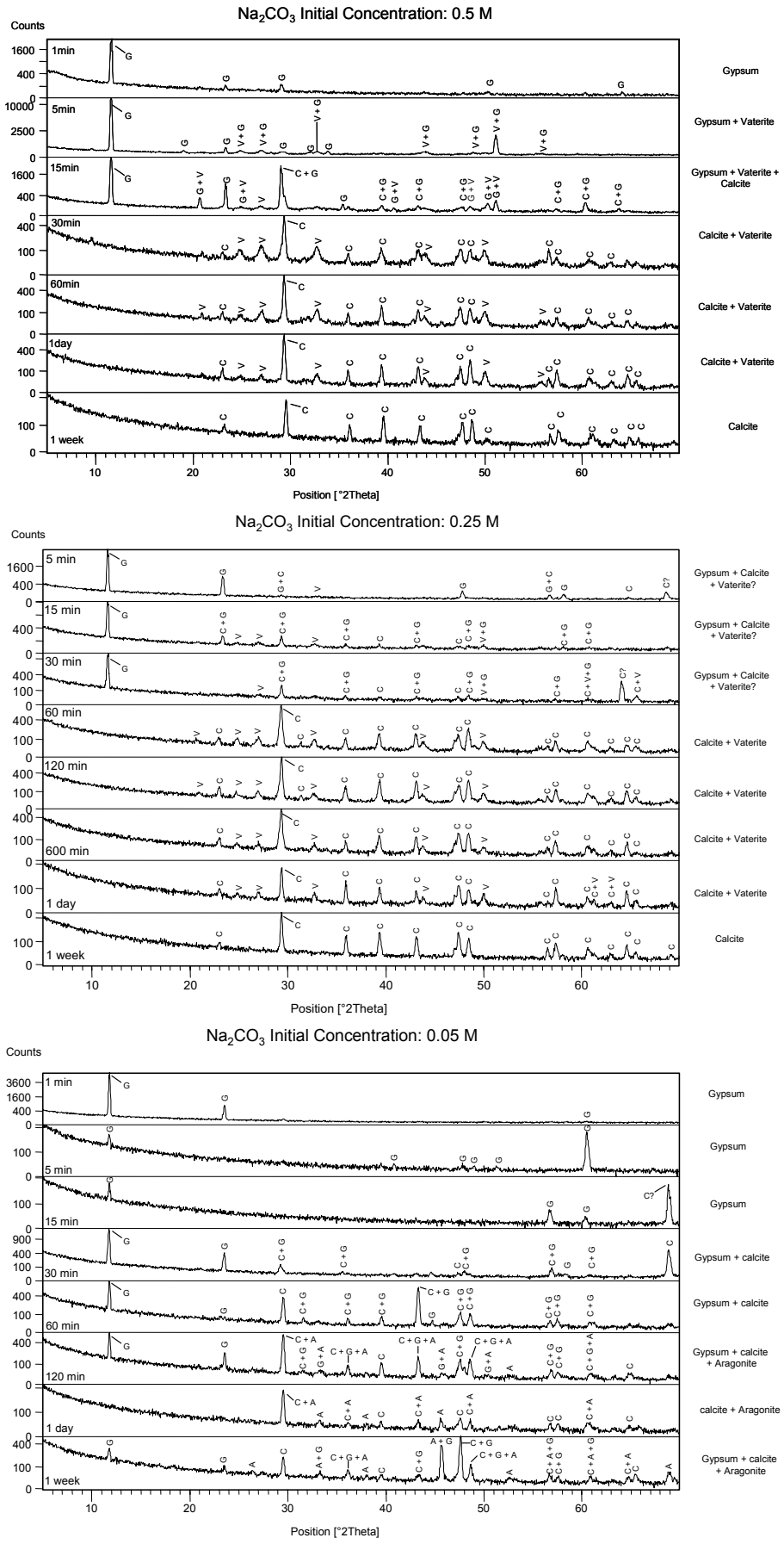

FIGURE 1. GIXRD diffraction scans recorded at 25 °C on gypsum (010) cleavage surfaces in contact with aqueous solutions with different Na_2CO_3 concentrations for specific periods of time. (**a**) 0.5 *M* Na_2CO_3, (**b**) 0.25 *M* Na_2CO_3, (**c**) 0.05 *M* Na_2CO_3. The X-ray diffraction patterns shown in **c** also illustrate a reaction sequence observed when a 0.1 *M* Na_2CO_3 aqueous solution was used. However, in the case of both 0.1 and 0.05 *M* Na_2CO_3 aqueous solutions, different reactions sequences were observed. In some, only calcite formed after ACC, whereas in others calcite was accompanied by either vaterite, aragonite, or both. G = gypsum; C = calcite; V = vaterite.

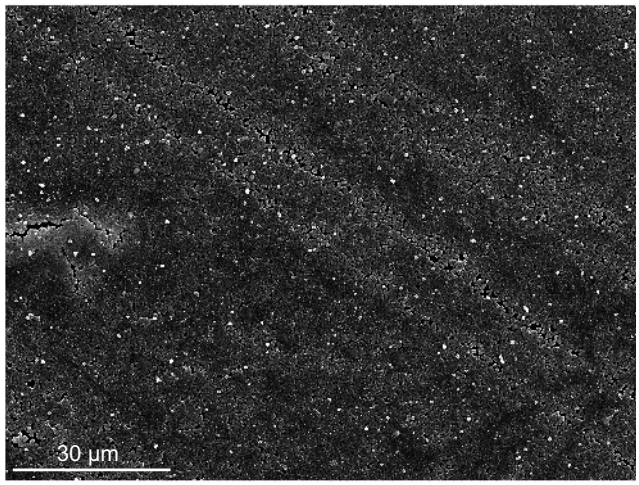

Figure 2. SEM micrograph showing the ACC layer that carpets the gypsum (010) surface after a 1 min reaction with a 0.5 *M* Na_2CO_3 aqueous solution. Note the parallel lines that reproduce the cleavage lines on the (010) surface of the original gypsum crystal.

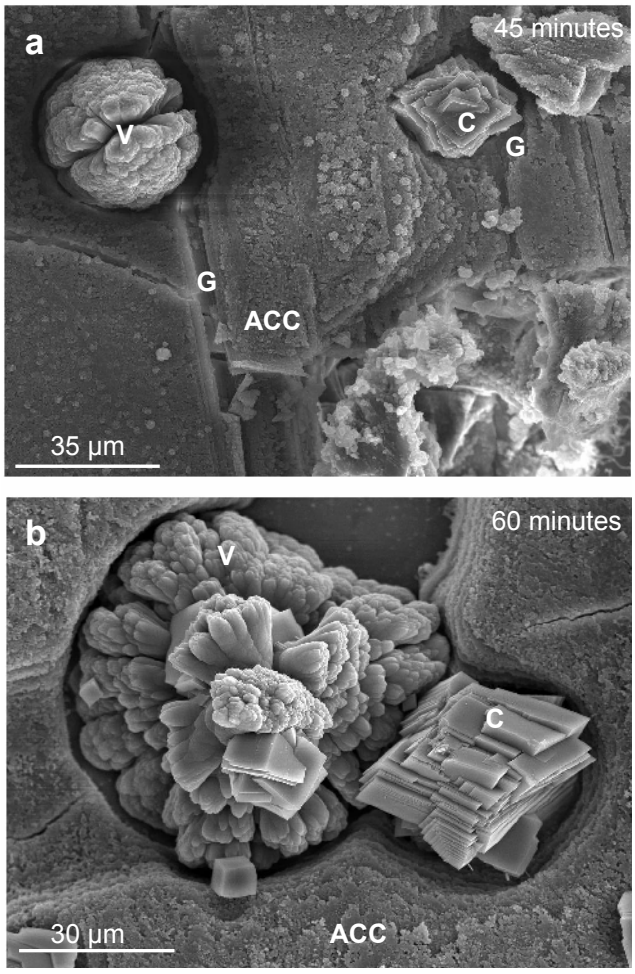

Figure 3. SEM micrographs showing the replacement of gypsum (G) and the ACC layer (ACC) by vaterite (V) and calcite (C). (**a**) The image has been taken of the original gypsum surface after a 45 min period in contact with a 0.5 *M* Na_2CO_3 aqueous solution. (**b**) The image corresponds to a reaction period of 60 min with a 0.5 *M* Na_2CO_3 aqueous solution. Note the growth of a calcite crystal against the surface of a vaterite spherulite.

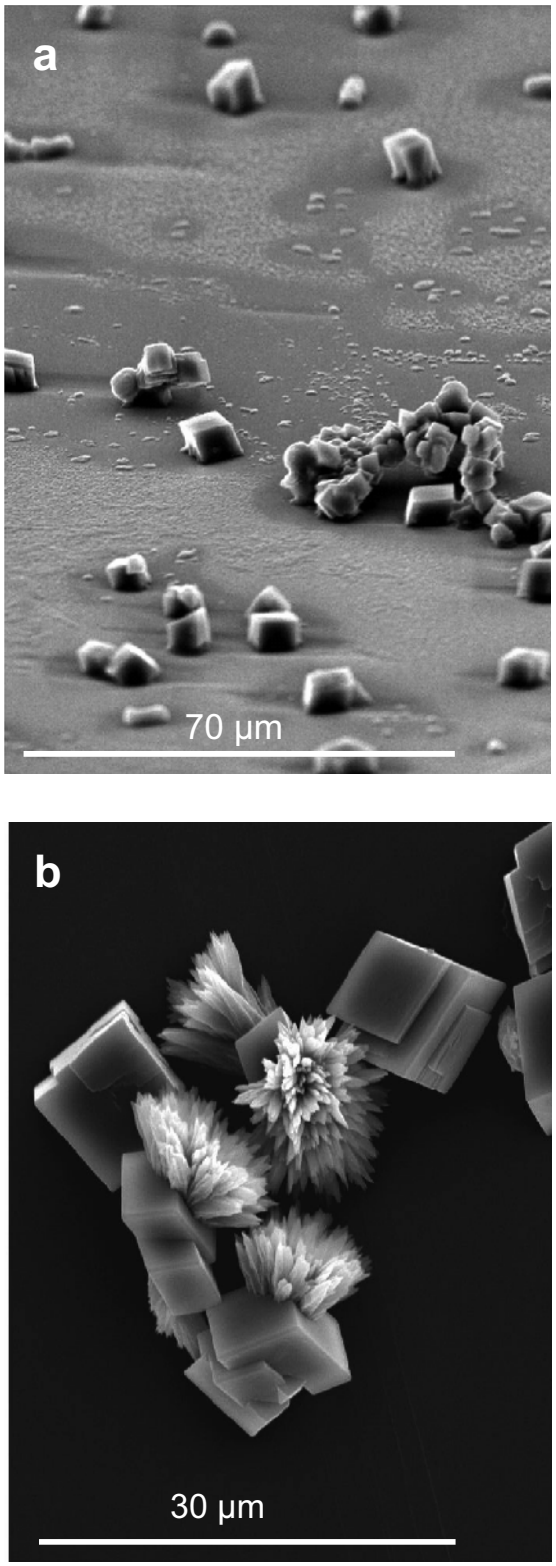

Figure 4. SEM micrographs showing (**a**) thin patches of ACC and calcite rhombohedra formed on the original gypsum (010) surface after a reaction period of 5 min. Note that the calcite crystals show flat and smooth $\{10\bar{1}4\}$ faces. (**b**) Calcite rhombohedra and aragonite spherulites showing the typical fibrous-radial morphology, formed after a reaction period of 15 min. In both cases, the concentration of the Na_2CO_3 aqueous solution was 0.05 *M*.

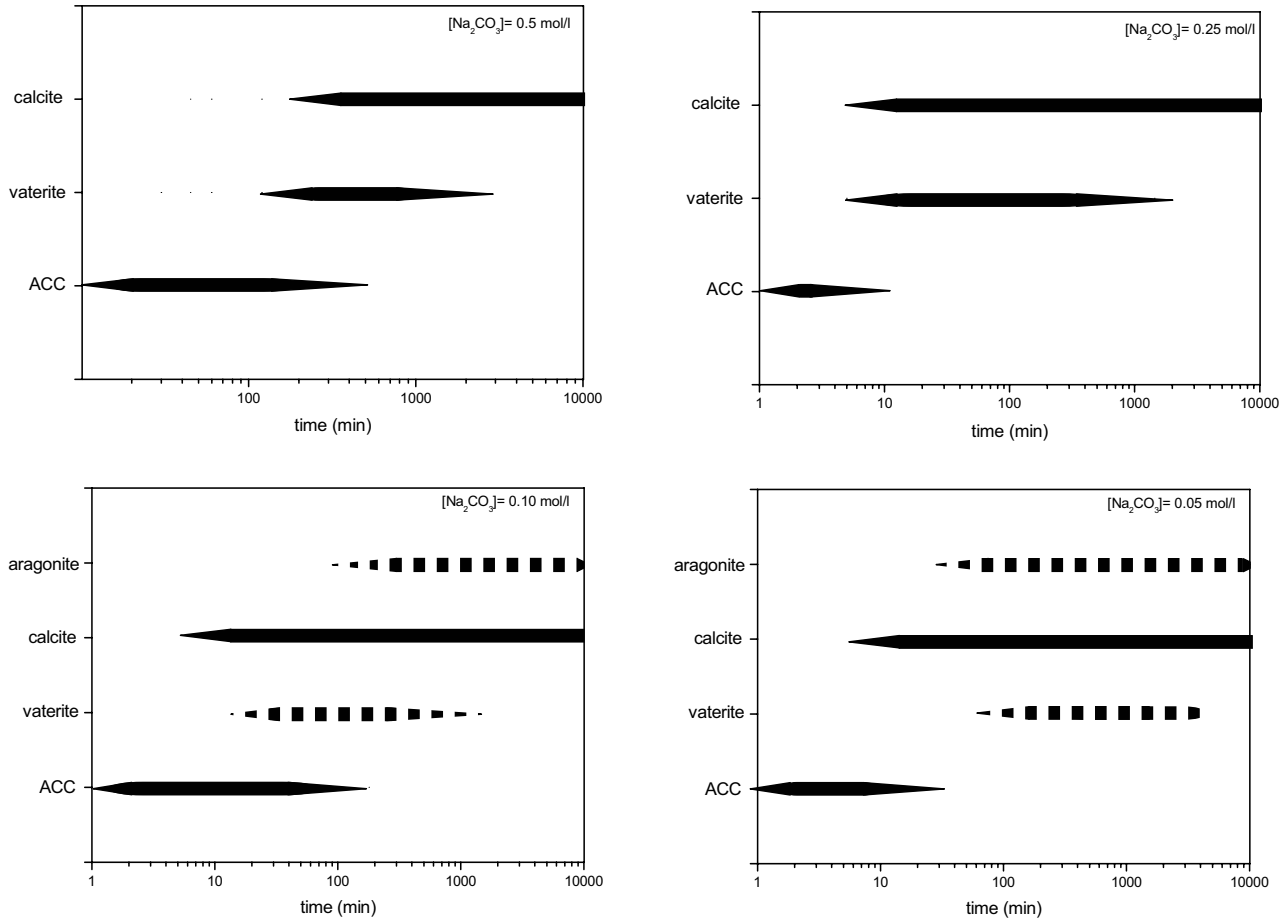

FIGURE 5. Schematic representation of the $CaCO_3$ phases in the replaced layer vs. time. Each graphic corresponds to a different initial concentration of the aqueous solutions of Na_2CO_3. The broken bands indicate that the corresponding phases do not always form.

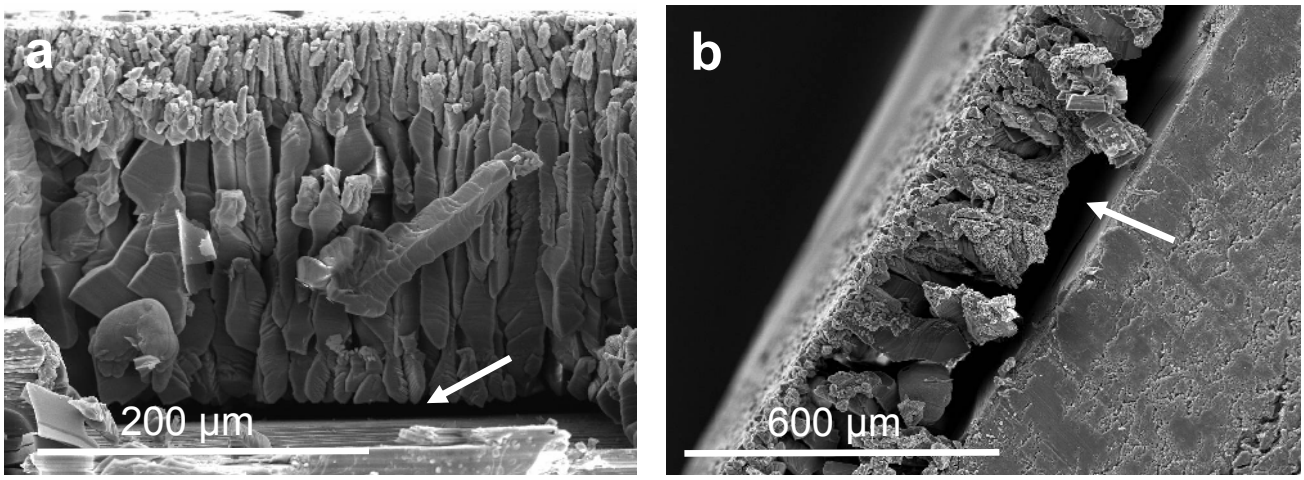

FIGURE 6. SEM micrographs showing the characteristics of the transformed layer, with the columns formed by calcite rhombohedra orientated perpendicular to the inward-moving gypsum surface. (**a**) After 300 min interaction with a 0.25 *M* Na_2CO_3 aqueous solution. (**b**) After 240 min in contact with a 0.5 *M* Na_2CO_3 aqueous solution. The images were taken on surfaces parallel to (100) or (001) in the original gypsum crystal.

solution is 0.25 *M*, the reaction sequence is very similar to that described above. However, the transformation of ACC into calcite and vaterite occurs much more rapidly. Thus, after a reaction period of 15 min, traces of ACC barely remain observable in the SEM images.

For solutions with lower starting carbonate concentrations (0.1 and 0.05 *M*) the sequence of reactions observed shows several distinctive features: (1) a less developed ACC layer, which appears as very thin patches randomly distributed on the gypsum surface and that rapidly dissolves in favor of the growth of calcite crystals from the very beginning of the reaction (reaction time ≤5 min). Moreover, calcite crystals have formed either on ACC or

directly on the gypsum surface (Fig. 4a). (2) After the formation of calcite, carbonatation may progress without the formation of any new phase. However, the formation of aragonite, vaterite, or both has been observed (in about a third of the experimental runs) after short reaction periods (15 min) (Fig. 4b). When these phases form, aragonite spherulites and vaterite aggregates coexist with calcite crystals during the first 24 h of the process. After a week in contact with the solution, calcite is the main phase in the transformed layer, vaterite is absent, and aragonite, although still distinguishable in both the X-ray diffraction diagrams and the SEM images, is not abundant.

Figure 5 schematically summarizes the sequence of formation of $CaCO_3$ phases vs. time for the different starting concentrations of carbonate in aqueous solution. As illustrated, the ACC lasts longer when the initial concentration of the solution is higher. In addition, the stable $CaCO_3$ phase calcite forms later in highly concentrated solutions. In the case of solutions with lower carbonate concentrations, calcite occasionally coexists with other metastable phases (vaterite and/or aragonite) for longer periods.

Some specific textural aspects of the replacement of gypsum crystals by calcite can be better observed on sections cut perpendicular to the (001) original surface. SEM images show that the transformed region consists of two layers. The outer-layer is very thin (15–20 μm) and consists of fine-grained calcite. In contrast, the inner-layer is thick and consists of columns of calcite rhombohedra oriented with their $\bar{3}$-axes approximately perpendicular to the original surface of the sample (Figs. 6a and 6b). Most interesting is the existence of a small gap between the inward-penetrating layer of $CaCO_3$ and the surface of the gypsum crystal, which is much more evident when aqueous solutions with a low carbonate concentration are used. Such a gap is indicated by arrows in Figures 6a and 6b. A clearer image of the relationship between the $CaCO_3$ layer and the gypsum "relict" is observed in Figure 7. The $CaCO_3$ layer appears continuous, encapsulating the gypsum crystal, and highly porous (Fig. 7a). In Figure 7b, a detail of the $CaCO_3$ layer, the gypsum surface and the small gap in between are shown. Note that the thickness of the $CaCO_3$ layer is not constant. Moreover, the differences in thickness are specially marked for different surfaces, due to their different reactivity. As mentioned above, we have focused on the advance of the replacement parallel to (010) because this is the face that dominates the morphology of most natural gypsum crystals.

PSEUDOMORPHISM

Carbonatation of gypsum leads to the formation of pseudomorphs. Although, in all the experiments conducted, the degree of faithfulness achieved in the reproduction of the characteristics of the original gypsum surface is quite coarse, some differences are evident depending on the starting carbonate concentration in the aqueous solution. Such differences are, in turn, a consequence of the characteristics of the outer-layer in the transformed crystals. Thus, when the starting carbonate concentration in the solution is 0.5 *M*, cleavage lines present on the original gypsum (010) surface can be preserved. Moreover, pseudomorph faces appear relatively smooth (Fig. 8a). When less concentrated solutions are used, the pseudomorphs are less perfect and the transformation affects only up to 30% of the whole volume of the original gypsum crystal. Thus, in the case of 0.25 *M* Na_2CO_3 solutions, both the external shape and the volume of the original gypsum crystals are preserved, but not the surface detail. Moreover, the surface of the pseudomorphs is not smooth. Finally, when 0.1 or 0.05 *M* Na_2CO_3 solutions are used, the development of the replacement process is limited to the outermost region of the original gypsum crystal and the pseudomorphs are much less perfect than in either of the two previous cases considered (Fig. 8b). Therefore, it can be concluded that the higher the starting carbonate concentration of the solution, the more faithful the pseudomorphs obtained.

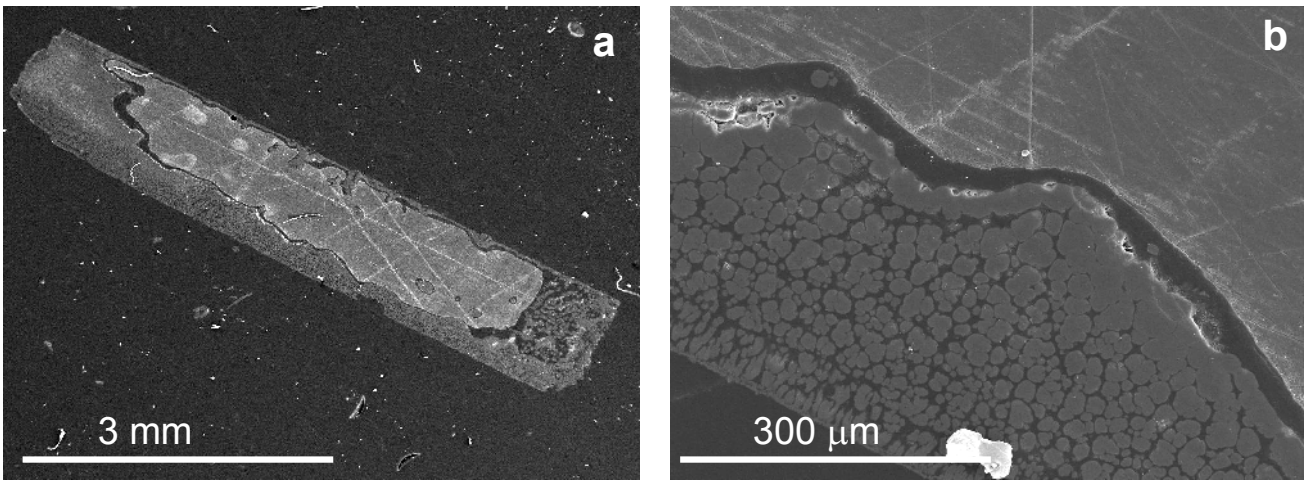

FIGURE 7. SEM micrographs of a polished section of a gypsum crystal partially replaced by $CaCO_3$. (**a**) General view of the relict of the original gypsum crystal, encapsulated within the porous $CaCO_3$ layer. Note that the advancement of the carbonatation front occurs more rapidly perpendicular to [010] than parallel to this direction. This is a consequence of the layer-like structure of gypsum, which causes the planes in the zone of the twofold axis to be more reactive than the (010) surface. (**b**) Detail showing the porosity of the $CaCO_3$ layer and the small gap developed in between this layer and the inward moving surface of the gypsum crystal.

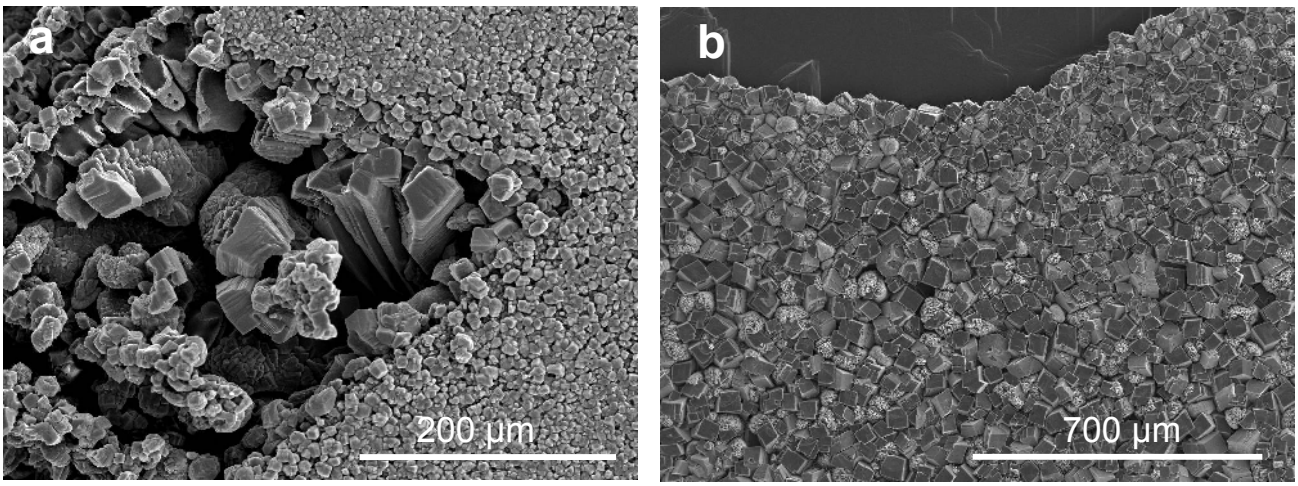

FIGURE 8. SEM micrographs showing the surface of the original gypsum fragment after a reaction period of one week. Na_2CO_3 concentration of the aqueous solution: (**a**) 0.5 *M* and (**b**) 0.05 *M*.

Advancement of the carbonatation front

Several measurements of the width of the transformed region after different reaction periods were carried out on SEM images of the partially carbonated gypsum crystals cut perpendicular to their (010) surface. These measurements are shown in Figure 9. As illustrated, the width of the $CaCO_3$ layer rapidly increases with time during the early stages of the process. Later, in all cases, the rate of advance of the carbonatation front decreases. When 0.5 *M* Na_2CO_3 aqueous solutions are used, the entire gypsum crystal transforms into $CaCO_3$ in a relatively short period of time. However, in the remainder of the cases, the time elapsed between the beginning of the process and the virtual end of the transformation depends on the starting carbonate concentration in the solution. Thus, the higher the concentration, the longer a high carbonatation rate is maintained. When the starting carbonate concentration in the solution is 0.25 *M*, the replacement front moves forward rapidly for ~300 min, but almost no advancement is observed for longer reaction periods. Finally, in the case of 0.1 and 0.05 *M* Na_2CO_3 solutions, the rapid advancement of the carbonatation front is restricted to the very initial stages of the process, almost completely stopping for reaction periods over 200 min.

DISCUSSION

Mineralogical evolution during the carbonatation process

The transformation of gypsum into $CaCO_3$ through reaction with carbonate-bearing aqueous solutions is especially complex since it involves the formation of one amorphous [ACC ($Ksp_{ACC} = 10^{-6.0}$) (Ogino et al. 1987)] and three crystalline polymorphs of $CaCO_3$ (vaterite, aragonite, and calcite [$Ksp_{calcite} = 10^{-8.48}$, $Ksp_{aragonite} = 10^{-8.336}$, $Ksp_{vaterite} = 10^{-7.91}$ (Plummer and Busenberg 1982)]. In the experiments presented, the dissolution-crystallization processes observed can be described as a series of solvent-mediated transformations (Cardew and Davey 1985) and are the inevitable consequence of the thermodynamic drives toward minimizing the free energy of the system in the most efficient way, i.e., at the maximum rate (Nicolis 1989). As soon as a gypsum crystal is in contact with a carbonate solution, it begins to dissolve and, as a result, Ca^{2+} and SO_4^{2-} ions are released to the solution. Thus, the solution rapidly becomes supersaturated with respect to all $CaCO_3$ solid phases mentioned above, at least in the vicinity of the interface between the aqueous solution and the gypsum surface. Although calcite is the stable polymorph of $CaCO_3$ at room temperature and the supersaturation with respect to this phase will be always ~300× higher than for ACC, in all the experiments the ACC is the first phase to nucleate. As Levi-Kalisman et al. (2000) pointed out, amorphous materials are characterized by the lack of certain properties rather than by their presence. This is particularly obvious in the case of ACC. Recent investigations by Michel et al. (2008) have highlighted that there exists a variety of ACC, both anhydrous and hydrated, most commonly with H_2O:$CaCO_3$ ratios around 1, which can also show different degrees of "stabilization." It is beyond the scope of this work to carry out a characterization of the amorphous phase that forms during the initial stages of the reaction. Therefore, ACC is used here without implying specific characteristics of hydration or stability. As indicated by Sawada (1998), the formation of ACC is promoted by kinetic factors. This behavior is in agreement with the predictions of the Ostwald Law of Stages, which states that the nucleation of most soluble and disordered phases is kinetically favored (Söhnel and Garside 1992). Experimental evidence of rapid nucleation of ACC from highly supersaturated solutions, as well as of its role as a precursor of more stable crystalline forms, have been found and discussed by different authors (Bolze et al. 2002; Pontoni et al. 2003). Nucleation of ACC occurs directly on the surface of the gypsum crystal rather than in the aqueous solution. This may be due to both the significant reduction of the activation energy that nucleation on a substrate represents in comparison to homogeneous nucleation (Chernov 1984) and the fact that supersaturation at the interface between the gypsum crystal and the solution is likely to be higher than in the aqueous solution. As pointed out by different authors (Stumm and Morgan 1985; Wang and Morse 1996), heterogeneous nucleation is the primary mechanism for mineral formation from aqueous solution in natural environments. The

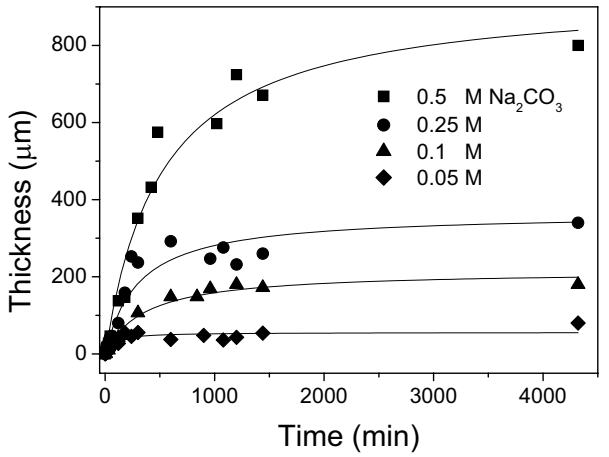

FIGURE 9. Thickness of the transformed layer as a function of time. Data corresponding to the four different Na_2CO_3 concentrations are plotted.

formation of ACC makes the supersaturation decrease. However, a solution in equilibrium with ACC is still supersaturated with respect to other less soluble $CaCO_3$ polymorphs. This situation constitutes the driving force for the simultaneous dissolution of ACC and the nucleation and growth of other $CaCO_3$ phases. This dissolution-crystallization process proceeds simultaneously with the progress of gypsum dissolution and starts soon after the beginning of the experiments (≈30 min for 0.5 *M* and 5 min for 0.25, 0.1, and 0.05 *M*), only ending when the ACC layer has completely disappeared. The different crystallization sequences observed, depending on the starting carbonate concentration in the solution, can be related to differences in the supersaturation level for the polymorphs of $CaCO_3$ during the initial stages of the transformation processes. It is evident that at the initial stages, supersaturation is higher when more concentrated carbonate solutions are used (Na_2CO_3 0.5 and 0.25 *M*). Thus, when the carbonate concentration is high, the progress of gypsum dissolution maintains a high supersaturation with respect to other $CaCO_3$ phases even after the formation of the ACC layer. This promotes the nucleation of metastable vaterite. Finally, a further reduction of supersaturation resulting from the growth of vaterite favors the nucleation of the stable phase calcite. In contrast, when less concentrated solutions are used (0.1 and 0.05 *M*), the supersaturation decrease, a consequence of the formation of the ACC layer, readily leads to the nucleation of calcite. Although the differences in the mineralogical sequence observed as a result of the starting carbonate concentration are evident, in all the cases several dissolution-crystallization loops, characteristic of solvent-mediated transformations, are simultaneously operating during the carbonatation process.

As has been explained previously, vaterite and/or aragonite crystals frequently form after the nucleation of calcite when low carbonate concentrations are used. This seems to indicate that the very high SO_4^{2-}/CO_3^{2-} ratios in the solution contribute to promote the crystallization of both vaterite and aragonite with respect to calcite. The formation of aragonite and/or vaterite after calcite nucleation always occurs very soon (reaction time ~15 min), when the carpeting of the gypsum surface is still very limited. It can be assumed that under these conditions the solution film directly in contact with the crystal surface approaches saturation with respect to gypsum. This means that the SO_4^{2-}/CO_3^{2-} ratio will be higher in the case of aqueous solutions with lower carbonate concentrations. Our observation is consistent with the results reported by Bischof and Fyfe (1968) and Bischof (1968), who found that SO_4^{2-} ions promote the formation of aragonite with respect to calcite and have a retarding or inhibiting effect on the transformation of vaterite into aragonite and of aragonite into calcite via solution. Moreover, a connection between the formation of metastable vaterite in nature and the presence of high concentrations of SO_4^{2-} ions in the crystallization media has also been proposed by several authors (Lippmann 1973; Grasby 2003). On the other hand, it is worth noting that aragonite lasts longer than vaterite in the transformed layer. This may be related to the slight difference in solubility between calcite and aragonite, which leads to a very low driving force and, consequently, more sluggish kinetics for the solvent-mediated transformation of aragonite into calcite.

Textural characteristics and pseudomorphism

The textural characteristics of the transformed layer, shown in Figure 6, are consistent with the advance of a carbonatation front into the gypsum crystals. There is particularly strong evidence of this in the orientation of the columns of calcite rhombohedra within the transformed layer. Such columns can be identified as soon as calcite becomes the dominant phase in the replacement and, in them, the rhombohedra show their threefold axis oriented perpendicular to the original surface of the reactant crystal. Moreover, these calcite crystals show signs of dendritic growth pointing to the inward-moving surface of the gypsum crystal. Therefore, it indicates that the carbonatation can be described as a process of mass-transfer through an interfacial fluid film from the gypsum surface to the $CaCO_3$ layer.

Another aspect that deserves consideration is the faithfulness of the pseudomorphs formed after the replacement of the original gypsum crystals by a $CaCO_3$ aggregate. A higher degree of faithfulness is obtained when gypsum crystals react with solutions with a higher carbonate concentration. When the concentration is high, the nucleation of the replacing phase ACC occurs immediately, forming a thin layer that completely carpets the gypsum surface, reproducing most of its original features. Moreover, the subsequent transformation of the ACC into vaterite and calcite via solvent also occurs under high supersaturation conditions, which causes the formation of a high number of small crystals. Measurements of the calcite crystals' size formed on the original gypsum surface after extended reaction periods (longer than 24 h) give an average value of ≈5 μm when the starting carbonate concentration in the aqueous solution is 0.5 *M*. The small size of the crystals is the reason that the pseudomorphs obtained in this case show smooth surfaces and that a higher degree of faithfulness in the reproduction of the details of the original surface is achieved.

In contrast, when the starting carbonate concentration in the solution is lower, a more significant volume of the original gypsum crystal needs to dissolve before the critical supersaturation for the nucleation of the new phase is reached. In fact, for 0.1 and 0.05 *M* Na_2CO_3 aqueous solutions, ACC never forms a

homogeneous layer, but appears as discontinuous patches that do not completely cover the surface of the gypsum crystal. This causes a partial loss of the original textural information of the substrate. Moreover, the nucleation occurs under lower supersaturation conditions and a smaller number of nuclei of calcite form on the gypsum surface. The growth of these nuclei leads to the development of crystals much larger (calcite crystals' average size ≈90 μm) than in the case described above. This explains the reduction of the pseudomorphs' faithfulness.

It is worth mentioning that the reproduction of fine morphological details of the original surface is also favored by the random crystallographic orientation of the calcite crystals. Pöml et al. (2007) have pointed out the importance of the lack of epitaxial relationships in the transfer of surface information during a replacement process.

Advancement of the carbonatation front

Some general conclusions about the factors that control the coupling of the dissolution and crystallization reactions involved in the carbonatation of gypsum can be extracted from the kinetic data previously reported in the results section. The fact that in all the cases considered, the carbonatation kinetics is characterized by an initial region in which the transformation front advances rapidly, followed by a progressive slowdown of its front advancement rate, seems to indicate that the general kinetics of the process is independent of the sequence of phase transformations occurring within the transformed region. Moreover, in all cases a reasonably linear relationship between the thickness of the $CaCO_3$ layer and time$^{1/2}$ exists, as is evidenced by plots presented in Figure 10. Therefore, it must be concluded that, at least during the initial stages of the carbonatation process, the advancement of the carbonatation front is controlled by the diffusion of the reactant from the solution bulk to the interface between the $CaCO_3$ layer and the gypsum crystal (Lasaga 1998). The subsequent slowdown of the carbonatation rate can be interpreted as a consequence of the interplay of at least three main factors: (1) the formation of a thick layer of $CaCO_3$ that partially precludes the percolation of the solution toward the gypsum surface; (2) the depletion of the solution in CO_3^{2-}, which reduces the concentration of the reactants' gradient; and (3) the increase in the SO_4^{2-}/CO_3^{2-} ratio during the process. This interpretation is supported by the results of the simulations of the physicochemical evolution of the system, carried out using the geochemical code PHREEQC. These simulations show that, for the time at which the carbonatation front advancement stops, in none of the cases considered has the bulk aqueous solution reached equilibrium with respect to gypsum (see Fig. 11). Moreover, the concentration of carbonate ions in the solution is still high enough to guarantee the precipitation of $CaCO_3$ if the dissolution of gypsum progressed, as can be observed in Figure 12. Consequently, the driving force for the progress of carbonatation still persists when it stops.

It is evident that the thickening of the transformed layer strongly contributes to the slowdown of the carbonatation progress. Moreover, the armoring effect of the newly formed layer becomes more important as the process advances. However, the preservation of the original volume of the gypsum crystal during the process requires the generation of microporosity.

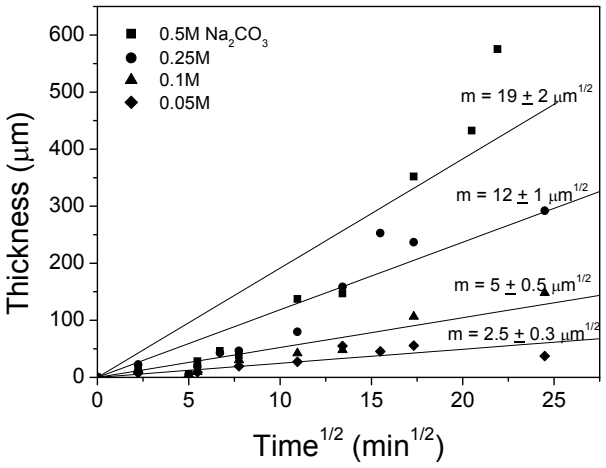

FIGURE 10. Thickness of the transformed layer as a function of time$^{1/2}$. Data corresponding to the four different Na_2CO_3 concentrations are plotted. The fits of the data to linear functions, as well as the values of the slopes of the lines, are shown.

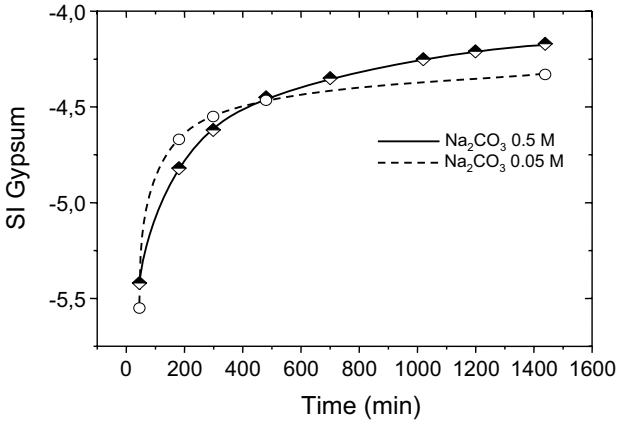

FIGURE 11. Comparison between the estimates of the evolution of the saturation index (SI) for gypsum of the aqueous solutions with starting carbonate concentrations of 0.5 and 0.05 *M*.

This is a general behavior when either the molar volume or the solubility of the product or both are smaller than those of the reactant phase (Yanagisawa et al. 1999; Glikin et al. 2003; Putnis and Mezger 2004; Putnis and Pollok 2004; Putnis et al. 2005; Putnis and Putnis 2004, 2007; Suárez-Orduña et al. 2004; Rendón-Ángeles et al. 2006; Pöml et al. 2007). In the case under consideration, the differences between the molar volumes of the $CaCO_3$ phases and gypsum are very significant (34.2 cm^3/mol for aragonite, 36.40 cm^3/mol for calcite, 56.5 cm^3/mol for vaterite, and 74.5 cm^3/mol for gypsum). Moreover, the solubility of gypsum is much higher than the solubility of any of the $CaCO_3$ phases considered (around 1000 times higher than calcite's). As a result, the amount of gypsum dissolved is much more than the amount of $CaCO_3$ precipitated (Putnis et al. 2005). Therefore, the volume reduction cannot be only balanced by the generation of microporosity. This situation is solved by the development of the observed gap between the inward-moving gypsum surface and the $CaCO_3$ layer. This gap is occupied by the interfacial liquid,

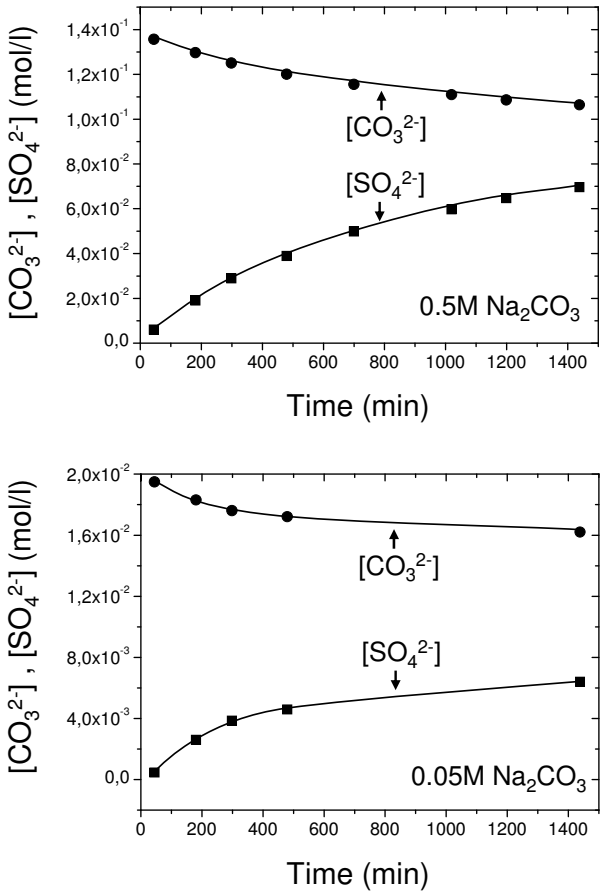

FIGURE 12. Estimate of the chemical evolution of the aqueous solution, considering the change in CO_3^{2-} concentration and SO_4^{2-} concentration: (**a**) solution 0.5 *M* Na_2CO_3, (**b**) solution 0.5 *M* Na_2CO_3.

which communicates with the surrounding solution through the newly formed microporosity. It is worth pointing out that the gap between the $CaCO_3$ layer and the gypsum surface, and thus the volume of the interfacial liquid, increases as the carbonatation progresses. This is a consequence of the fact that as the transformation progresses, the difference between the volume of gypsum that has dissolved and the volume of solid newly formed increases, i.e., the volume reduction that needs to be compensated increases. Moreover, for an equivalent volume of carbonatation, such a gap will be higher when the initial carbonate concentration in the solution is lower, in agreement with our observations (Fig. 6). This can be explained considering that when solutions with a low concentration are used, a much higher amount of gypsum needs to be dissolved before the interfacial liquid reaches a supersaturation that guaranties the progress of calcite crystal growth. The development of a similar gap between the inward moving surface of the reactant phase and the product has been previously observed and discussed by Pöml et al. (2007) for the replacement of pyrochlore as a result of hydrothermal alteration. In the case under consideration, the progress of the transformation is also favored by the absence of crystallographic relationships between the gypsum substrate and the product phases. As Prieto et al. (2003) demonstrated, the formation of epitaxial layers can rapidly armor a substrate and lead to the virtual stoppage of the dissolution-crystallization process, while a connected porosity net develops when epitaxial relationships are absent. The existence of both microporosity and the layer of liquid filling the gap at the interface should guarantee the progress of the carbonatation process at a relatively high rate. However, this is not supported by the observations. Therefore, other factors must play an important role in the evolution of the carbonatation kinetics. The most likely explanation for the inconsistency between the expected evolution of the carbonatation rate and our observations is a progressively reduced permeability of the $CaCO_3$ layer as time goes on, as a consequence of both the compositional and textural re-equilibration. The closing of porosity after replacement as a result of textural re-equilibration has been observed in the case of some simple systems (Putnis et al. 2005). Such evolution of the porosity has been interpreted as being driven by the reduction of interfacial area. A similar process could occur in the system under consideration. To achieve a general conclusion on this particular aspect will require carrying out a detailed study of the microtextural characteristics of the $CaCO_3$ layer and their evolution, which will be addressed in a forthcoming work.

CONCLUDING REMARKS

The carbonatation of gypsum crystals in contact with carbonate-bearing aqueous solutions occurs through several dissolution-crystallization reactions that involve the formation of several $CaCO_3$ metastable polymorphs (ACC, vaterite, aragonite) and their solvent-mediated transformation into the stable phase calcite. The reaction pathway depends on the initial concentration of carbonate in the aqueous solution, which also determines the degree of faithfulness in the reproduction of the original characteristics of the surface of the original gypsum crystal. Higher carbonate compositions yield more faithful reproductions. The carbonatation progresses due to the development of microporosity during the process, which guarantees the diffusion of the reactant to the interface between the gypsum surface and the $CaCO_3$ layer. Such microporosity is a consequence of the difference in both molar volume and solubility between gypsum and the $CaCO_3$ phases involved. The kinetics of the carbonatation front advancement is also controlled by the carbonate concentration of the aqueous solution, as well as by the formation of microporosity. The carbonatation progresses rapidly during the initial stages and its rate is controlled by the diffusion of the reactant from the bulk solution to the interface between the gypsum surface and the $CaCO_3$ layer. A subsequent slowdown of the carbonatation rate can be concluded to be a consequence of several factors: the general chemical evolution of the system, the thickening of the transformed layer, its textural re-equilibration, etc. The results presented here show that the experimental study of dissolution-crystallization reactions occurring in nature can provide relevant information to improve our current understanding of the processes involved in the development of mineral replacement phenomena. Moreover, reaching a more accurate knowledge of the factors controlling the transfer of textural information during replacement can be especially important to draw conclusions on both fossilization and biomineralization.

ACKNOWLEDGMENTS

The authors are grateful to two anonymous reviewers for their valuable comments. We are also indebted to the Associate Editor, Ian Swainson, for his helpful suggestions. We sincerely thank Eugenio Baldonedo, from the Microscopy Centre-UCM, for assistance and support with the SEM, and Emilio Matesanz, from the X-ray Diffraction Central Service-UCM, for technical support and help in GIXRD interpretation. Financial support through the Spanish Ministry of Science and Innovation (Project CGL2007-65523-CO2-01) and the Comunidad de Madrid (Project CAM-2006 910148) is gratefully acknowledged. The Spanish Ministry of Education and Science has also financially supported to Nuria Sánchez-Pastor (Postdoctoral fellowship).

REFERENCES CITED

Anadón, P., Rosell, L., and Talbot, M.R. (1992) Carbonate replacement of lacustrine gypsum deposits in two Neogene continental basins, eastern Spain. Sedimentary Geology, 78, 201–216.

Bell, C.M. (1989) Saline lake carbonates within a Jurassic-Lower Cretaceous continental red bed sequence in Atacama region of northern Chile. Sedimentology, 36, 651–663.

Bischof, J.L. (1968) Catalysis, inhibition, and the calcite-aragonite problem. I. The vaterite-aragonite transformation. American Journal of Science, 266, 65–79.

Bischof, J.L. and Fyfe, W.S. (1968) Catalysis, inhibition, and the calcite-aragonite problem. II. The aragonite-calcite transformation. American Journal of Science, 266, 80–90.

Bolze, J., Peng, B., Dingenouts, N., Panine, P., Narayanan, T., and Ballauff, M. (2002) Formation and growth of amorphous colloidal $CaCO_3$ precursor particles as detected by time-resolved SAXS. Langmuir, 18, 8364–8369.

Cañaveras, J.C., Sánchez-Moral, S., Calvo, J.P., Hoyos, M., and Ordoñez, S. (1996) Dedolomites associated with karstification, an example of early dedolomitization in lacustrine sequences from the Tertiary of the Madrid Bassin, Central Spain. Carbonate and Evaporites, 11, 85–103.

Cañaveras, J.C., Sánchez-Moral, S., Sanz-Rubio, E., and Hoyos, M. (1998) Meteoric calcitization of magnesite in Miocene lacustrine deposits (Calatayud Basin, NE Spain). Sedimentary Geology, 119, 183–194.

Cardew, P.T. and Davey, R.J. (1985) The kinetics of solvent-mediated phase transformations. Proceedings of the Royal Society of London, Series A, 398, 415–428.

Carmichael, D.M. (1969) On the mechanism of prograde metamorphic reactions in quartz-bearing pelitic rocks. Contributions to Mineralogy and Petrology, 20, 244–267.

Chernov, A.A. (1984) Modern Cystallography III: Crystal Growth, 517 p. Springer-Verlag, Berlin.

Flörke, W. and Flörke, O.W. (1961) Vateritbildung aus Gips in Sodalösung. Neues Jahrbuch für Mineralogie, Monatschaften, 179–181.

Glikin, A.E., Kovalev, S.I., Rudneva, E.B., Kryuchkova, L.Yu., and Voloshin, A.E. (2003) Phenomena and mechanisms of mixed crystal formation in solutions I. General concept on the example of the system $KHC_8H_4O_4$-RbH $C_8H_4O_4$-H_2O. Journal of Crystal Growth, 255, 150–162.

Grasby, S.E. (2003) Naturally precipitating vaterite (μ-$CaCO_3$) spheres: Unusual carbonates formed in an extreme environment. Geochimica et Cosmochimica Acta, 67, 1659–1666.

Harlov, D.E., Wirth, R., and Hetherington, C.J. (2007) The relative stability of monazite and huntonite at 300–900 °C and 200–1000 MPa: Metasomatism and the propagation of metastable mineral phases. American Mineralogist, 92, 1652–1664.

Kirkland, D.W. and Evans, R. (1976) Origin of Limestones Buttes, Gypsum Plain, Cultherson County, Texas. American Association of Petroleum Geologists Bulletin, 60, 2005–2018.

Lasaga, A.C. (1998) Kinetic Theory in Earth Sciences, 728 p. Princeton University Press, New Jersey.

Levi-Kalisman, Y., Raz, S., Weiner, S., Addadi, L., and Sagi, I. (2000) X-Ray absorption spectroscopy studies on the structure of a biogenic "amorphous" calcium carbonate phase. Journal of the Chemical Society, Dalton Transactions, 3977–3982.

Lippmann, F. (1973) Sedimentary Carbonate Minerals, 229 p. Springer-Verlag, Berlin.

McKenzie, J.A., Hsú, K.J., and Schneider, J.F. (1980) Movement to subsurface waters under the sabkha, Abu Dhabi, U.A.E., and its relationship to evaporative dolomite genesis. In D.H. Zenger, J.B. Dunham, and R.L. Ethington, Eds., Concepts and Models of Dedolomitization, 28, p.11–30. Society of Economic Paleontologists and Mineralogists Special Publication, Tulsa.

Michel, F.M., MacDonald, J., Feng, J., Phillips, B.L., Ehm, L., Tarabrella, C., Parise, J.B., and Reeder, R.J. (2008). Structural characteristics of synthetic amorphous calcium carbonate. Chemistry of Materials, 20, 4720–4728.

Nicolis, G. (1989) Physics of far-from-equilibrium systems and self-organisation. In P. Davies, Ed., The New Physics, 11, p. 316–347, Cambridge University Press, U.K.

Oelkers, E.H., Putnis, C.V., and Putnis, A. (2007) Do fluids flow through or around mineral grains? Geochimica et Cosmochimica Acta, 71, A729.

Ogino, T., Suzuki, T., and Sawada, K. (1987) The formation and transformation mechanism of calcium carbonate in water. Geochimica et Cosmochimica Acta, 51, 2757–2767.

Parkhurst, D.L. and Appelo, C.A.J. (2000) User's guide to PHREEQC (version 2). A computer program for speciation, batch-reaction, one-dimensional transport, and inverse geochemical calculations. U.S. Geological Survey Water-Resources Investigations Report, p. 99–4259.

Pierre, C. and Rouchy, J.M. (1988) Carbonate replacements after sulphate evaporates in the Middle Miocene of Egypt. Journal of Sedimentary Petrology, 58, 446–456.

Pina, C.M., Fernández-Díaz, L., Prieto, M., and Putnis, A. (2000) In situ observations of a dissolution-crystallisation reaction: The phosgenite-cerussite transformation. Geochimica et Cosmochimica Acta, 64, 215–221.

Plummer, L.N. and Busenberg, E. (1982) The solubilities of calcite, aragonite and vaterite in CO_2-H_2O solutions between 0 and 90 °C, and an evaluation of the aqueous model for the system $CaCO_3$-CO_2-H_2O. Geochimica et Cosmochimica Acta, 46, 1011–1040.

Pöml, P., Menneken, M., Stephan, T., Niedermeier, D.R.D., Geisler, T., and Putnis, A. (2007) Mechanism of hydrothermal alteration of natural self-irradiated and synthetic crystalline titanate-based pyrochlore. Geochimica et Cosmochimica Acta, 71, 3311–3322.

Pontoni, D., Bolze, J., Dingenouts, N., Narayanan, T., and Ballauff, M. (2003) Crystallization of calcium carbonate observed in-situ by combined small- and wide-angle X-ray scattering. The Journal of Physical Chemistry B, 107, 5123–5125.

Prieto, M., Cubillas, P., and Fernández-González, A. (2003) Uptake of disolved Cd by biogenic aragonite: A comparison with sorption onto calcite. Geochimica et Cosmochimica Acta, 67, 3859–3869.

Putnis, A. (2002) Mineral replacement reactions: from macroscopic observations to microscopic mechanism. Mineralogical Magazine, 66, 689–708.

Putnis, A. and Putnis, C.V. (2004) Reactive fronts at the nanoscale: The nature and origin of a coupled dissolution-precipitation interface. Geochimica et Cosmochimica Acta, 68, A180.

——— (2007) The mechanism of reequilibration of solids in the presence of a fluid phase. Journal of Solid State Chemistry, 180, 1783–1786.

Putnis, A., Niedermeier, D.R.D., and Putnis, C.V. (2006) From epitaxy to topotaxy: The migration of reaction interfaces through crystals. Geochimica et Cosmochimica Acta, 68, A166.

Putnis, C.V. and Mezger, K. (2004) A mechanism of mineral replacement: Isotope tracing in the model system KCl-KBr-H_2O. Geochimica et Cosmochimica Acta, 68, 2839–2848.

Putnis, C.V. and Pollok, K. (2004) Porosity development in replacement reactions: NaCl-KCl-H_2O as a model example. Geochimica et Cosmochimica Acta, 68, A166.

Putnis, C.V., Tsukamoto, K., and Nishimura, Y. (2005) Direct observation of pseudomorphism: compositional and textural evolution at a fluid-solid interface. American Mineralogist, 90, 1909–1912

Putnis, C.V., Austrheim, H., and Putnis, A. (2007a) A mechanism of fluid transport through minerals. Geochimica et Cosmochimica Acta, 71, A814.

Putnis, C.V., Geisler, T., Schmid-Beurmann, P., Stephan, T., and Giampaolo, C. (2007b) An experimental study of the replacement of leucite by analcime. American Mineralogist, 92, 19–26.

Rendón-Ángeles, J.C., Pech-Canul, M.I., López-Cuevas, J., Matamoros-Veloza, Z., and Yanagisawa, K. (2006) Differences on the conversion of celestite in solutions bearing monovalent ions under hydrothermal conditions. Journal of Solid State Chemistry, 179, 3645–3652.

Rouchy, J.M., Bernet-Rollande, M.C., and Maurin, A. (1994) Descriptive petrography of evaporites: applications in the field, subsurface and the laboratory. In The Evaporitic Series in Petroleum Exploration, 1: Geological Methods, p. 70–123. Technip, Paris.

Rouchy, J.M., Taberner, C., Blanc-Valleron, M.M., Sprovieri, R., Russell, M., Pierre, C., Di Stefano, E., Pueyo, J.J., Caruso, A., Dinarés, J., Gomis-Coll, E., Cespuglio, G., Wolff, G., Ditchfield, P., Santisteban, C., Pestrea, S., Comboureu-Nebout, N., Santisteban, S., and Grimalt, J.O. (1998) Sedimentary and diagenetic markers of the restriction in a marine basin: The Lorca basin (SE Spain) during the Messinian. Sedimentary Geology, 121, 23–55.

Rouchy, J.M., Taberner, C., and Peryt, T.M. (2001) Sedimentary and diagenetic transitions between carbonates and evaporites. Sedimentary Geology, 140, 1–8.

Sánchez-Pastor, N., Pina, C.M., and Fernández-Díaz, L. (2007) A combined in situ AFM and SEM study of the interaction between celestite (001) surfaces and carbonate-bearing aqueous solutions. Surface Science, 601, 2973–2982.

Sanz-Rubio, E., Sánchez-Moral, S., Cañaveras, J.C., Calvo, J.P., and Rouchy, J.M. (2001) Calcitization of Mg-Ca carbonate and Ca sulphate deposits in a continental Tertiary basin (Calatayud Basin, NE Spain). Sedimentary Geology, 140, 123–142.

Sawada, K. (1998) Mechanisms of crystal growth of ionic crystals in solution. Formation, transformation, and growth inhibition of calcium carbonates. In H.

Ohtaki, Ed., Crystallization Processes, p. 39–68. Wiley, New York.
Simon, B. and Bienfait, M. (1965) Structure et méchanisme de croissance du gypse. Acta Crystallographica, 19, 750–756.
Söhnel, O. and Garside, J. (1992) Precipitation, 391 p. Butterworth-Heinemann, Oxford.
Stumm, W. and Morgan, J.J. (1985) Aquatic Chemistry. Wiley, New York.
Suárez-Orduña, R., Rendón-Ángeles, J.C., López-Cuevas, J., and Yanagisawa, K. (2004) The conversion of mineral celestite to estrontianite under alkaline hydrothermal conditions. Journal of Physics: Condensed Matter, 16, S1331–S1344.
Wang, Q.W. and Morse, J.W. (1996) Pyrite formation under conditions approximating those in anoxic sediments. 1. Pathway and morphology. Marine Chemistry, 52, 99–121.
Wang, Y., Wang, Y., and Merino, E. (1995) Dynamic weathering model: Constraints required by coupled dissolution and pseudomorphic replacement. Geochimica et Cosmochimica Acta, 59, 1559–1570.
Wigley, T.M.L. (1973) Chemical evolution of the system calcite-gypsum-water. Canadian Journal of Earth Sciences, 10, 306–315.
Yanagisawa, K., Rendón-Ángeles, J.C., Ishiwara, N., and Oishi, S. (1999) Topotaxial replacement of chlorapatite by hydroxyapatite during hydrothermal ion exchange. American Mineralogist, 84, 1861–1869.
Youssef, E.A.A. (1989) Geology and genesis of sulphur deposits at Ras Gemsa area, Red Sea Coast, Egypt. Geology, 17, 797–801.